PUBLICATIONS OF THE
ASTRONOMICAL SOCIETY OF THE PACIFIC

Vol. 72 | October 1960 | No. 428

A SURVEY OF GALACTIC RADIATION AT 960 MC/S

R. W. Wilson and J. G. Bolton
California Institute of Technology Radio Observatory
Owens Valley, California

I. INTRODUCTION

Observations have been made of galactic radiation at a frequency of 960 Mc/s with an antenna of 0°.8 beam width over a range of 300° in galactic longitude. The beam width used is comparable to that used by Hill, Slee, and Mills at 85 Mc/s,[1] and by Westerhout at 1390 Mc/s.[2] The present survey has considerably greater coverage than either of these and sufficient overlap to permit a reasonable study of the variation of the brightness distribution with frequency.

The observations are presented as a series of contour maps on equal-area charts. Data are given on the 110 discrete sources observed, including their positions, flux densities, angular sizes and, where possible, spectra and identifications.

II. THE OBSERVATIONS

The 960 Mc/s receiving system used for this survey was that described by Harris and Roberts.[3] The comparison radiometer was switched alternately between the feed horn and a reference resistor immersed in liquid nitrogen. An output time constant of one second was used throughout. About half of the survey was made by driving across the sky at a rate of one degree per minute with the antenna on a series of fixed declinations. South of $\delta = -40°$ the observations were made with the antenna stationary, in order to avoid the effects of varying ground radiation. North of $\delta = +40°$ the antenna was set on a given right ascension and driven north at the rate of one degree per minute. These three methods are referred to in Table I as α drives, α drifts, and δ drives.

TABLE I

TYPE AND SPACING OF OBSERVATIONS

Figure	Region	Type of Observation	Average Spacing of Observations
2	16^h00^m to 18^h20^m	α drift below −40°	0°.5
	−48° to −30°	α drive above −40°	
3	17^h00^m to 19^h40^m	α drive	0°.6
	−30° to 0°		
4	18^h00^m to 21^h00^m	α drive	0°.5 from 0° to +20°
	0° to +30°		1°.0 from +20° to +30°
5	19^h30^m to 21^h15^m	α drive	0°.7
	+30° to +60°		
6	21^h00^m to 1^h00^m	δ drive	7^m
	+40° to +70°		
7	1^h00^m to 5^h00^m	δ drive	7^m
	+40° to +70°		
8*a*	4^h30^m to 7^h00^m	α drive	1°.5
	0° to +40°		
8*b*	6^h00^m to 8^h00^m	α drive	1°.5
	−40° to 0°		
9	8^h00^m to 9^h30^m	α drift	0°.5
	−48° to −40°		

The spacing of the successive observations in right ascension or declination was determined by the complexity of the region involved. Table I gives the method of observation and the spacings relevant to the various sections of the survey.

The observations were carried out over a period of four months between July and November, 1959, and for the greater part of the survey were made not more than two hours from the meridian. All of the observations were made at night. For each region a series of long records in which a zero baseline was evident was made at intervals of approximately five degrees. These records were then used to determine the coverage necessary for the intermediate observations.

Calibration of the flux density, or antenna-temperature scale, was made from an observation on each night of M 87 or, when this was not possible, one of Cygnus A or Cassiopeia A. The ratios of the flux densities of these sources were taken from Harris and Roberts, and, following them, the flux density of M 87 was assumed as 300×10^{-26} watts $m^{-2}(c/s)^{-1}$. Night-to-night variations of a few percent occurred in the observed flux densities of the calibration sources; however, we have used averages over the separate observing periods in the belief that the stability of the receiver parameters was better than the individual source observations indicated. Dial corrections for the antenna pointing were also obtained from the observations of Harris and Roberts.

III. REDUCTION OF THE OBSERVATIONS

An example of an actual record is given in Figure 1. In reducing the observations, we drew a zero baseline in on each record with the help of the long records described earlier. Then a series of parallel lines was drawn on the record representing the adopted contour intervals. The right ascensions or declinations of the intersections of the contour parallels and the observed profiles were then read off the record and plotted as points on equal-area charts (scale 2 cm = 1°). The contours of Figures 2 to 9 were steered through the plotted points. Finally the coordinate system was

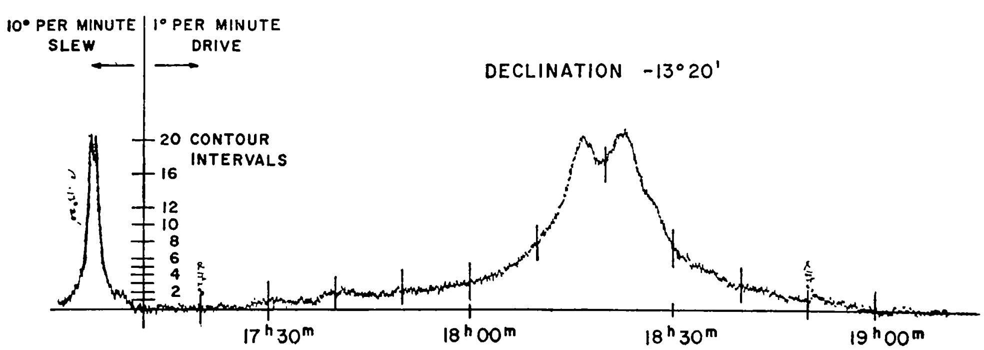

FIG. 1.—Sample record of an observation at $\delta = -13°20'$, made by driving the antenna at a rate of one degree per minute.

corrected for the effects of telescope-pointing errors and for precession to the standard epoch of 1950. The large-scale maps were photographically reduced and redrawn. The galactic equator (on the old system) is shown as a dashed line.

Corrections were applied for refraction where they were in excess of 2′, but no corrections were made for extinction at low altitudes of observation.

On the scale of the contour intervals M 87 gives a deflection of 24 units. For a flux density of 300×10^{-26} watts $m^{-2}(c/s)^{-1}$ and an (assumed) antenna efficiency of 50%, the antenna temperature due to M 87 is 30° K. Thus, the contours represent steps of 1°.25 K in observed antenna temperature above the zero baseline determined as described. The temperature of this residual level was not measured, but is probably of the order of 0°.5 K. The accuracy of the final contour maps is estimated at 10% or half a contour interval, whichever is the greater.

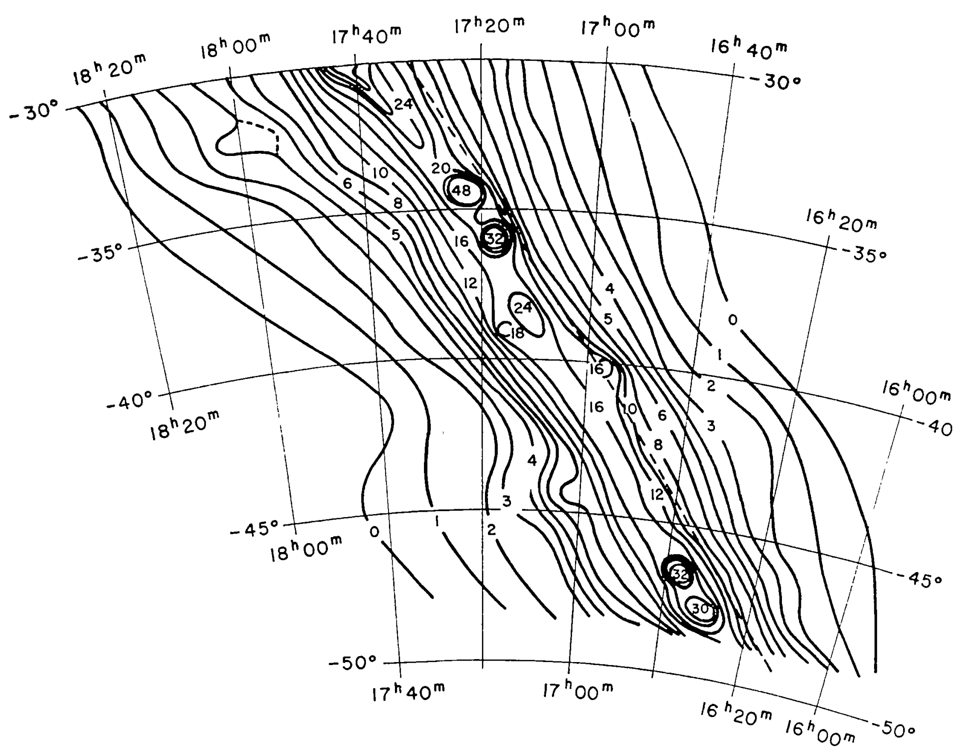

Fig. 2—Equal-area chart of the brightness distribution of the galactic radiation at 960 Mc/s, $\alpha = 16^h$ to 18^h20^m.

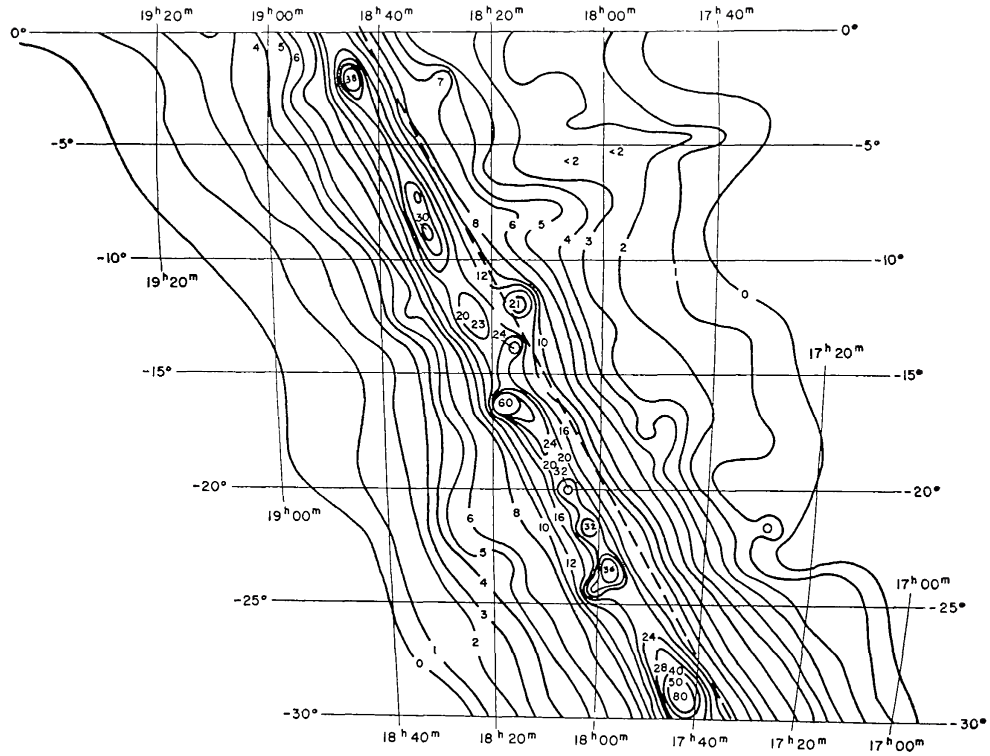

FIG. 3.—Equal-area chart of the brightness distribution of the galactic radiation at 960 Mc/s, $\alpha = 17^h$ to 19^h20^m.

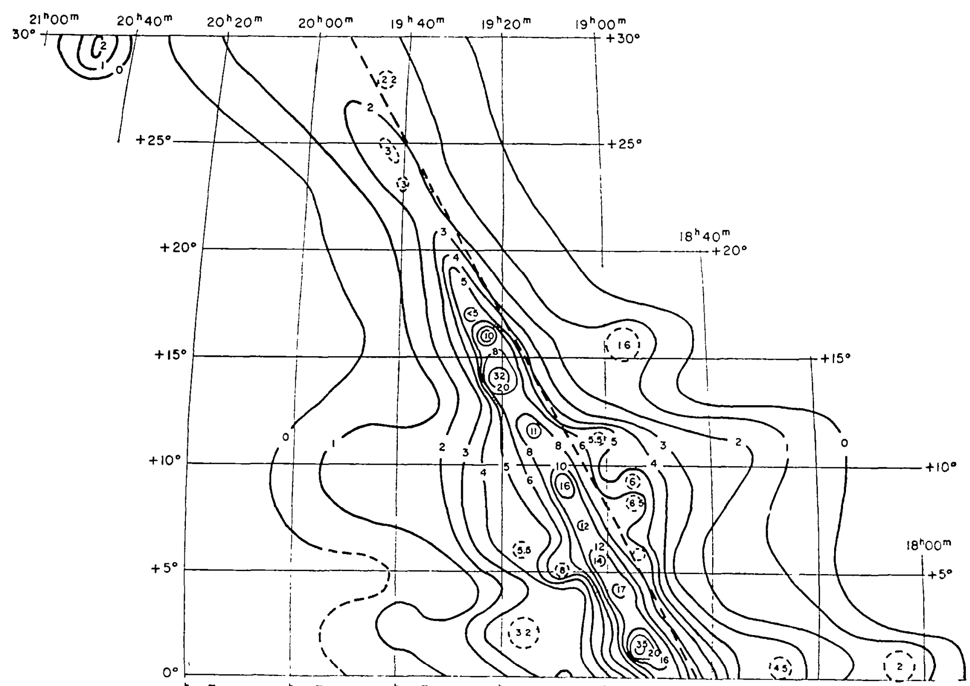

FIG. 4.—Equal-area chart of the brightness distribution of the galactic radiation at 960 Mc/s, $\alpha = 18^h$ to 21^h.

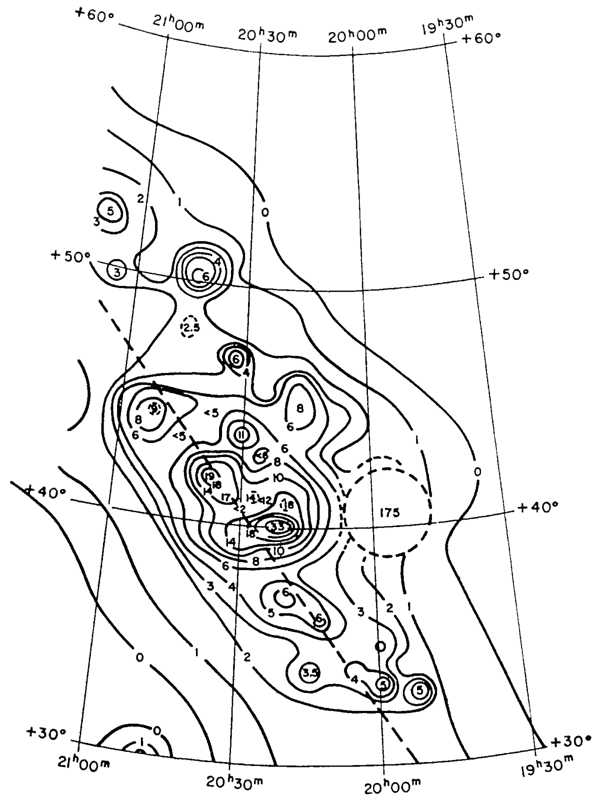

FIG. 5.—Equal-area chart of the brightness distribution of the galactic radiation at 960 Mc/s, $\alpha = 19^h30^m$ to 21^h.

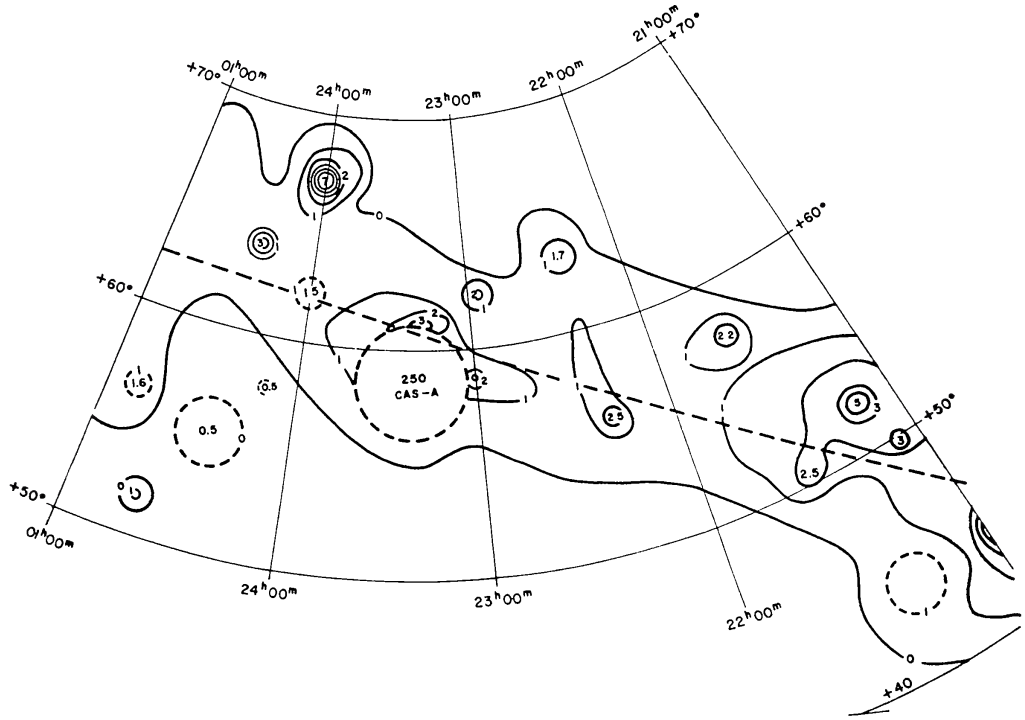

FIG. 6.—Equal-area chart of the brightness distribution of the galactic radiation at 960 Mc/s, $\alpha = 21^h$ to 1^h.

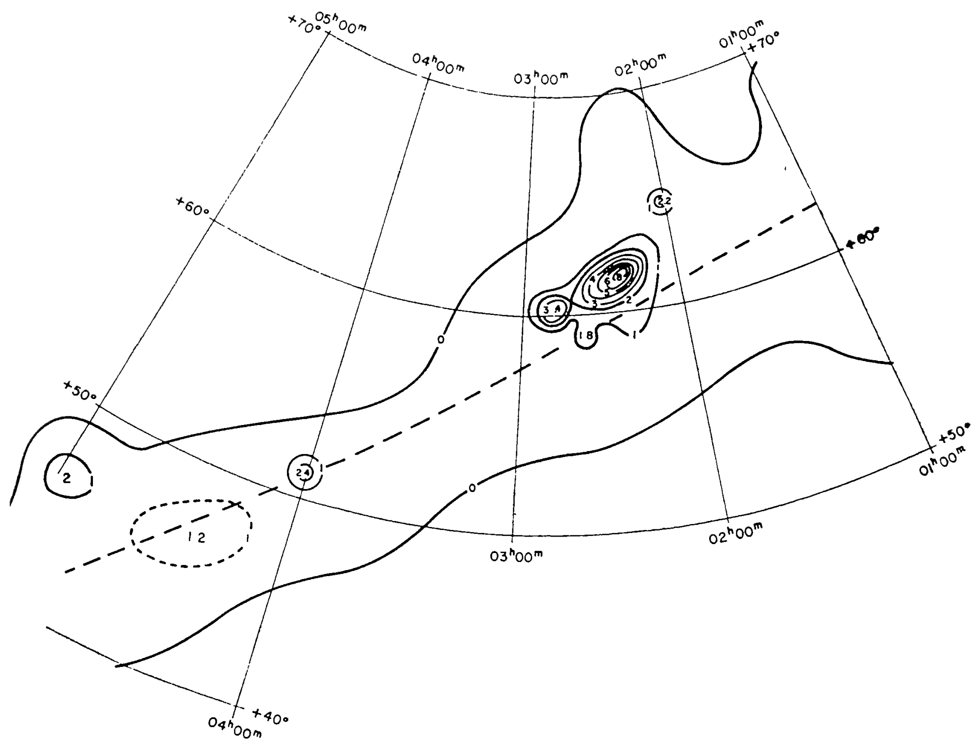

FIG. 7.—Equal-area chart of the brightness distribution of the galactic radiation at 960 Mc/s, $\alpha = 1^h$ to 5^h.

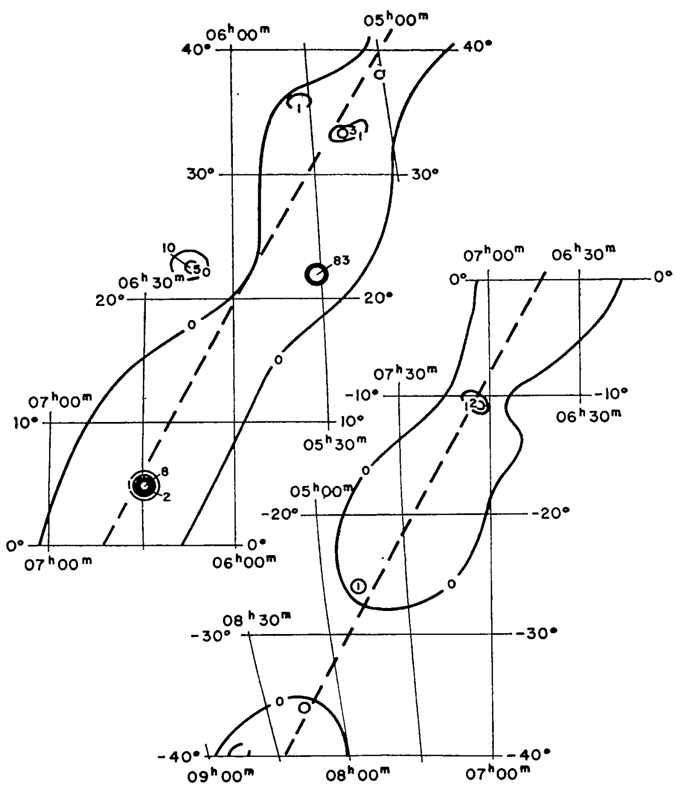

FIG. 8.—Equal-area chart of the brightness distribution of the galactic radiation at 960 Mc/s, $\alpha = 5^h$ to 9^h.

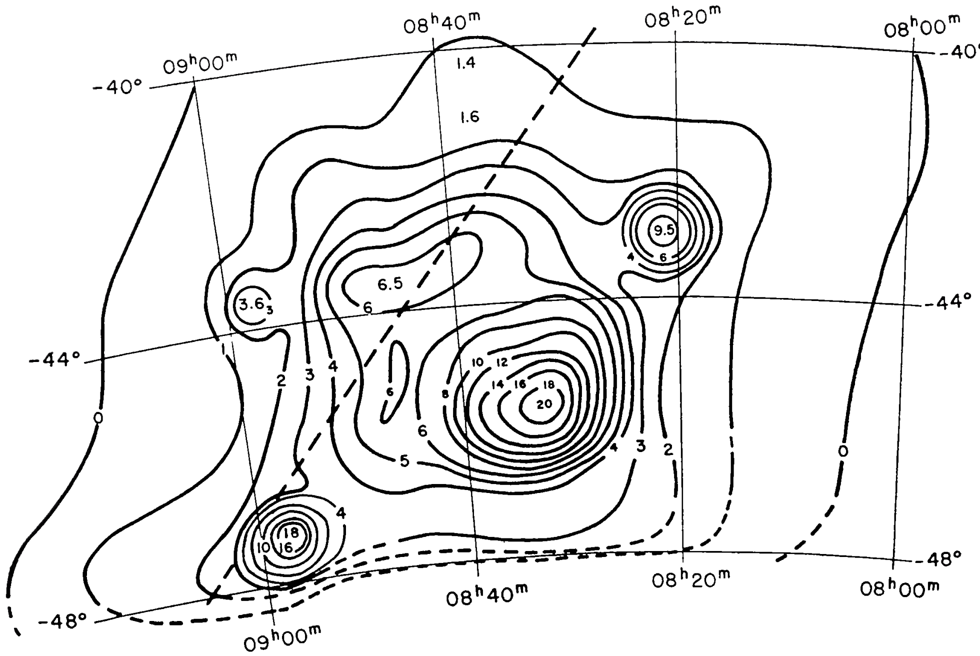

FIG. 9.—Equal-area chart of the brightness distribution of the galactic radiation at 960 Mc/s, $\alpha = 8^h$ to 9^h.

IV. THE SOURCE LIST

Table II contains a list of the 110 discrete sources observed in the survey. Approximately 60% of the objects have been catalogued by other observers, including some by Harris and Roberts. Neither the positions of the sources nor their flux densities deduced from the contour maps have very high accuracy, so that when better data were available from Harris and Roberts they have been used (noted by a plus sign in Table II). The figures in parentheses beside the values for right ascension and declination are indicative of the accuracy of the positions; there is a 75% chance that the source lies within the respective error limits:

(1)	± 2′,	(4)	± 20′,
(2)	± 4′,	(5)	> 20′.
(3)	± 10′,		

Where the sources are of large angular diameter and have no well-defined center (5) is used.

The flux densities given in column 4 are in units of 10^{-26} watts $m^{-2}(c/s)^{-1}$. The smaller values refer to the peak flux density, and the values in parentheses refer to an estimate of the integrated flux density in cases in which the sources are extended.

Estimates of the angular extent of the sources are given in column 5. For part of the survey and for the sources larger than $0\overset{\circ}{.}5$, the apparent widths to half-power points were determined from the contour maps. The values quoted in the table were deduced on the assumption that the sources have a Gaussian brightness distribution. For the range of longitudes from 100° through 360° to 30°, supplementary observations were made with two 90-foot antennas used as an interferometer with effective baselines of 134, 173, or 200 wavelengths. The sources observed with the interferometer are marked (I) in column 5 beside the angular sizes that were again deduced on the assumption of Gaussian brightness distributions. In certain cases, there was obvious conflict between the observations and this assumption. Such sources are noted in the "Remarks" column, where a simple interpretation of the results is given in such terms as "strong central concentration" or "fine structure." The deduced half-widths of the sources were used in computing the integrated flux densities of column 4, except for source No. 26, where a planimeter was used on the contour map. Several other sources were checked using this method. Column 6 gives the spectrum of the source wherever possible. The symbols used are:

T (Thermal). This indicates a spectrum in which the flux density is independent of wavelength, and is deduced from radio observations at three wavelengths or from observations at two radio wavelengths and a positive identification of the source with an emission nebula.

T? (Probably thermal). This is deduced from radio observations at only two wavelengths or from our own observation and a tentative identification of the source with an emission nebula.

NT (Nonthermal). This refers to sources where observations at two or more radio wavelengths show that the flux density increases approximately as ($\lambda^{0.7}$).

Sources have been classified only when they definitely fall into one of the above categories. For some sources, although an adequate number of observations was available, the evidence on the spectrum was inconclusive and no classification was made. A classification of thermal was assigned to 19 objects, probably thermal to 25, and definitely nonthermal to 15.

The notes list identifications or possible identifications with radio sources listed in other catalogues, and with objects visible on the 48-inch Schmidt plates. The designations used are:

HB—Hanbury Brown and Hazard[4];
HSM—Hill, Slee, and Mills[1];
MSH—Mills, Slee, and Hill[5];
W—Westerhout[2];
UOB—Müller[6];
3C—Edge, Shakeshaft, McAdam, Baldwin, and Archer[7];
R—Rishbeth[8];
Stromlo—Gum[9];
Sharpless—Sharpless[10].

Identifications with visible objects were possible for 44 sources. Of these, 34 are emission nebulae of which 15 already had identifications. Eight others have previously been identified as supernova remnants, and it is likely that two more are also supernova remnants. One of these, No. 26, shows a filamentary structure similar to that of Shaĭn 147, and it is possible that sources Nos. 28 and 29 are part of this object, which is heavily obscured on the following side. The other, source No. 13, does not have filamentary structure, but is similar to HB 9 and to an object found by Harris and Roberts (CTA 1).

This work was supported by the U. S. Office of Naval Research under contract Nonr–220(19).

---

[1] E. R. Hill, O. B. Slee, and B. Y. Mills, *Aust. J. Phys.,* **11,** 530, 1958.
[2] G. Westerhout, *B.A.N.,* **14,** 215, 1958 (No. 488).
[3] D. E. Harris and J. A. Roberts, *Pub. A.S.P.,* **72, 237,** 1960.
[4] R. Hanbury Brown and C. Hazard, *M.N.R.A.S.,* **113,** 123, 1953.

[5] B. Y. Mills, O. B. Slee, and E. R. Hill, *Aust. J. Phys.*, **11**, 360, 1958.
[6] H. G. Müller, *Pub. Bonn Obs.* No. 52, 1959.
[7] D. O. Edge, J. R. Shakeshaft, W. B. McAdam, J. E. Baldwin, and S. Archer, *Mem. R.A.S.*, **68**, 37, 1959.
[8] H. Rishbeth, *Aust. J. Phys.*, **11**, 550, 1958.
[9] C. S. Gum, *Mem. R.A.S.*, **67**, 155, 1955.
[10] S. Sharpless, *Ap. J. Supplements*, **4**, 257, 1959 (No. 41).
[11] K. G. Henize, *A.J.*, **64**, 51, 1959.
[12] B. Westerlund, private communication.

TABLE II

960 Mc/s Source List B

No.	α (1950)		δ (1950)		Flux Density		Size	Spectrum
1	0^h00^m3	(4)	+62°11′	(3)	19	(56)	~1°	
2	0 00.5	(3)	67 06	(2)	87	(220)	2° × 1°5	T
3	0 10.4	(4)	57 47	(4)	5		P?	
4	0 22.8	(1)+	63 51	(1)+	57+		P	NT
5	0 25.5	(5)	55 21	(5)	6	(48)	2° × 2°	
6	0 39.9	(2)+	51 47	(1)+	13+		P	NT
7	0 50.1	(2)+	56 20	(1)+	16+	(24)	~0°5	T
8	2 01.7	(1)+	64 36	(1)+	33+		5′(I)	T
9	2 23.7	(5)	61 43	(5)	98	(400)	1° × 2°5(I)	T
10	2 37.4	(4)	58 59	(4)	22	(25)	0°25(I)	
11	2 48.5	(3)	60 15	(3)	50	(175)	1°2 × 1°2(I)	T
12	4 00.8	(4)	51 12	(2)	30	(33)	1° × 2°5(I)	T
13	4 24	(5)	47 00	(5)	15	(225)	2° × 5°(I)	NT?
14	4 59	(3)+	46 25	(3)+	22+	(150)+	~2°	
15	5 01.2	(2)+	38 00	(2)+	15+		P	NT
16	5 12.4	(2)	33 48	(2)	25	(40)	~0°6(I)	T?
17	5 18.7	(2)	33 26	(2)	38	(60)	~0°7(I)	T
18	5 31.5	(1)+	21 59	(1)+	1030+		P	NT
19	5 37.1	(3)	36 00	(3)	13	(20)	~0°6	T?
20	6 14.3	(1)+	22 36	(4)+	129+	(195)+	~1°0(I)	NT
21	6 29.4	(2)+	+04 53	(2)+	105+	(342)+	~1°2(I)	T
22	7 03	(4)	−10 45	(4)	25	(125)	1°2 × 2°(I)	T?
23	7 48	(4)	−26 00	(4)	13	(?)		T?
24	8 15	(4)	−36 00	(4)	8	(?)		T?
25	8 21.4	(2)	−42 58	(3)	116	(187)	0°6 × 0°6(I)	NT
26	8 32.8	(3)	−45 37	(3)	238	(1400)	2° × 2°5(I)	
27	8 37.6	(5)	−40 34	(5)	13	(33)	1° × 1°(I)	T?
28	8 43	(5)	−43 31	(4)	19	(120)	2°5 × 1°5(I)	
29	8 45.7	(4)	−45 03	(5)	13	(40)	2° × 0°5(I)	
30	8 48.1	(5)	−42 15	(5)	13	(33)	1° × 1°(I)	T?
31	8 57.4	(2)	−47 16	(3)	200	(250)	0°5 × 0°25(I)	T?
32	8 57.8	(3)	−43 34	(4)	33	(59)	0°6 × 0°8(I)	T?
33	16 31.3	(3)	−47 42	(4)	172	(274)	0°6 × 0°7(I)	T?

NOTES TO TABLE II

No.	
1	Unidentified.
2	W 1, NGC 7822, emission nebula.
3	Unidentified.
4	HB 1, 3C 10, remnants of the supernova of A.D. 1572.
5	Unidentified.
6	3C 20, unidentified.
7	NGC 281, emission nebula.
8	3C 58, point source with unusual (flat) spectrum, heavy local obscuration.
9	W 3 + 4, IC 1795/1805, emission nebulae. Interferometer shows resolution into double object.
10	Unidentified, possibly 3C 69.
11	W 5, IC 1848, emission nebula.
12	IC 1491, emission nebula.
13	Possibly supernova remnant, nonfilamentary. Interferometer indicates fine structure.
14	HB 9, supernova remnant.
15	3C 134, unidentified point source, heavy local obscuration.
16	IC 405, emission nebula.
17	W 8, IC 410, emission nebula. Interferometer indicates central concentration.
18	Crab Nebula.
19	Sharpless 232, emission nebula.
20	IC 443, supernova remnant. Interferometer indicates fine structure.
21	Rosette Nebula, emission nebula.
22	Possibly NGC 2327/IC 2177, emission nebulae.
23	NGC 2467, emission nebula. Extended, but size observations inadequate.
24	NGC 2568 (NGC declination has 1° error), emission nebula. Extended, but size observations inadequate.
25	Puppis A, supernova remnant, point source plus extended source.
26	Vela X, supernova remnant similar to Shaĭn 147.
27	Stromlo 14, emission nebula.
28	Vela Y, R 58, probably part of Vela X.
29	Vela Z, R 59, probably part of Vela X.
30	Stromlo 17, emission nebula.
31	R 61, Stromlo 23. Interferometer indicates central concentration.
32	R 62, Stromlo 20. Interferometer indicates strong central concentration.
33	Position agrees with NGC 6164–5, an unusual planetary nebula[11] or H II region,[12] 7′ in extent; results doubtful owing to low altitude of observation. Interferometer indicates fine structure.

TABLE II (*Continued*)

960 Mc/s Source List B

No.	α (1950)		δ (1950)		Flux Density		Size	Spectrum
34	$16^h36^m.8$	(2)	−46°36′	(2)	185	(300)	0°.6 × 1° (I)	NT
35	16 56.7	(3)	−40 13	(3)	62	(66)	~0°.2 (I)	T?
36	17 01	(3)	−44 20	(3)	30		P?	
37	17 12.8	(3)	−38 03	(3)	86	(100)	0°.3 × 1°.5 (I)	NT
38	17 15.7	(3)	−39 00	(2)	37		8′ (I)	
39	17 17.7	(2)	−35 58	(2)	170	(180)	0°.2 (I)	T
40	17 23	(2)	−34 21	(2)	360	(540)	0°.6 (I)	T
41	17 28.7	(4)	−21 36	(4)	13		P	NT
42	17 42.9	(2)	−28 50	(2)	740	(1800)	1° × 1°.5 (I)	
43	17 48	(3)	−17 15	(4)	25	(35?)	>0°.5 (I)	
44	17 57	(4)	−32 15	(3)	12	(15?)	>0°.3 (I)	
45	17 57.8	(2)	−23 30	(3)	200	(240)	0°.25 × 0°.8 (I)	T
46	18 00.7	(3)	−24 21	(2)	100	(106)	0°.2 (I)	T
47	18 01.7	(2)	−21 39	(2)	150	(210)	~0°.5 (I)	NT
48	18 04.8	(4)	+00 40	(4)	12	(30)	~1° (I)	
49	18 06	(2)	−20 00	(3)	150	(165)	0°.25 (I)	NT
50	18 15.3	(2)	−12 00	(3)	140	(350)	1° × 1° (I)	T
51	18 16.2	(2)	−13 50	(3)	100	(106)	0°.2 (I)	T
52	18 17.5	(2)	−16 18	(2)	500		8′ (I)	T
53	18 23.5	(4)	−12 30	(4)	62	(200)	0°.5 × 2° (I)	T?
54	18 27.3	(2)	+00 30	(2)	19	(67)	~1.2° (I)	T?
55	18 28.6	(3)	−02 12	(3)	25	(26)	10′ (I)	
56	18 31.2	(2)	−08 45	(3)	75	(135)	0°.3 × 1°.3 (I)	T?
57	18 33.8	(2)	−07 15	(3)	50	(65)	16′ × 0°.6 (I)	T?
58	18 34	(3)	−12 12	(3)	12	(17)	~0°.5 (I)	
59	18 44.7	(2)	−02 06	(3)	315	(345)	0°.25 (I)	T?
60	18 53.6	(2)	+01 18	(2)	220	(240)	0°.25 (I)	NT
61	18 54.6	(2)	08 14	(3)	19	(22)	0°.3 (I)	T?
62	18 55	(3)	09 15	(3)	6			
63	18 56.4	(4)	15 37	(4)	14	(60)	~1°.5 (I)	
64	18 57.7	(2)	04 04	(3)	62	(87)	~0°.5 (I)	
65	19 01.0	(3)	05 32	(3)	25	(27)	0°.2 (I)	T?
66	19 01.4	(3)	11 14	(3)	12	(25)	~1° (I)	
67	19 04.6	(2)	07 12	(4)	25	(27)	9′ (I)	T?
68	19 07.9	(2)	09 02	(2)	100	(110)	0°.25 (I)	T?
69	19 08.4	(3)	05 04	(3)	25	(31)	0°.4 (I)	T?
70	19 13.8	(2)	11 36	(3)	37	(44)	0°.35 (I)	

NOTES TO TABLE II *(Continued)*

No.

34 HSM $l^{I} = 305^{\circ}.8$, unidentified. Interferometer indicates fine structure.

35 Uncatalogued emission nebula.

36 Unidentified.

37 HSM $l^{I} = 316^{\circ}.4$, extended to S.E., unidentified.

38 Unidentified.

39 NGC 6334, emission nebula.

40 W 22, NGC 6357, emission nebula. Interferometer indicates fine structure.

41 3C 358, remnant of supernova A.D. 1604.

42 Sagittarius A, galactic nucleus. Interferometer indicates central concentration.

43 MSH 17 − 110, unidentified.

44 Appears on Westerhout survey, but is not listed.

45 W 28, NGC 6514, M 20, emission nebula.

46 W 29, NGC 6523, M 8, emission nebula.

47 W 30, HSM $l^{I} = 334^{\circ}.2$.

48 Unidentified.

49 W 31, HSM $l^{I} = 336^{\circ}.4$, unidentified.

50 W 35, NGC 6604, emission nebula.

51 W 37, NGC 6611, emission nebula.

52 W 38, NGC 6618, M 17, extended to S.W., emission nebula.

53 W 39, unidentified.

54 MSH 18 + 05?, unidentified.

55 W 40, possibly heavily obscured emission nebula.

56 W 41, unidentified.

57 W 42, unidentified.

58 Unidentified.

59 W 43, unidentified. Interferometer shows point source superimposed on extended object.

60 W 44, MSH 18 + 011, 3C 392; interferometer shows point source superimposed on extended object.

61 W 45? Westerhout quotes as extended; unidentified.

62 W 46, Westerhout quotes as extended; unidentified.

63 Unidentified.

64 W 47, unidentified.

65 3C 396, unidentified.

66 Unidentified.

67 3C 397, unidentified.

68 W 49, 3C 398, unidentified.

69 W 50, MSH 19 + 01, unidentified.

70 Unidentified.

TABLE II (*Concluded*)

960 Mc/s Source List B

No.	α (1950)		δ (1950)		Flux Density		Size	Spectrum
71	$19^h15^m.7$	(5)	+02°05′	(5)	2	(12?)	2° ?(5)	
72	19 15.9	(3)	06 00	(3)	19	(23)	0°.35(I)	
73	19 20.7	(2)	14 04	(2)	320	(370)	0°.3?(I)	T?
74	19 22.8	(2)	16 00	(3)	50	(60)	0°.35(I)	
75	19 39	(5)	02 30	(5)	13	(70)	~1°.8(I)	
76	19 40	(2)	23 06	(3)	13	(15)	0°.3(I)	T
77	19 44	(4)	24 45	(4)	13	(20)	0°.3 × 1°(I)	
78	19 44.8	(3)	28 00	(3)	12	(15)	0°.35(I)	
79	19 46	(5)	09 30	(5)	13	(320)	~4°	
80	19 51.8	(2)	33	(3)	47	(130)	~1°.1	
81	19 57.7	(1)$^{+}$	40 36	(1)$^{+}$	2190^{+}		P	NT
82	19 59.2	(2)	33 24	(2)	31	(34)	0°.25	
83	19 59.4	(3)	35	(3)	13	(16)	0°.35	
84	20 05	(3)	34 06	(3)	13	(18)	~0°.5(I)	
85	20 12	(2)	36 05	(3)	36	(80)	~0°.9(I)	
86	20 14.3	(3)	33 55	(3)	13	(50)	~1°.5(I)	
87	20 14.3	(3)	37 03	(4)	10		P	
88	20 16.6	(5)	45 00	(5)	50	(200)	1°.0 × 1°.5	
89	20 19.5	(2)	40 52	(2)	63	(190)	~1°.0	
90	20 19.7	(2)	37 02	(3)	19	(120)	~1°.8	
91	20 21	(3)	40	(2)	250	(800)	0°.6 × 1°.8	T
92	20 27	(3)	41 10	(3)	31		P?	
93	20 30.4	(3)	43 48	(3)	60	(90)	0°.5 × 0°.6	T
94	20 32	(2)	39 30	(2)	63	(220)	~1°.2	
95	20 32.7	(2)	46 58	(3)	50	(100)	0°.6 × 1°.0	
96	20 37.5	(3)	41 55	(4)	160	(800)	~2°.0	
97	20 43.5^{+}	(2)	50 12^{+}	(2)	60^{+}	(186)$^{+}$	1°.3 × 1°.3	
98	20 45.2	(4)	48 03	(4)	6			
99	20 48.2^{+}	(5)	29 30^{+}	(5)	33^{+}	(252)$^{+}$	2° × 2°.5	
100	20 52.5	(5)	44 09	(5)	75	(350)	1°.5 × 2°	T
101	21 05.9	(3)	49 48	(3)	13		P	
102	21 10.6	(3)	52 16	(2)	38	(60)	1° × 1°	
103	21 20	(5)	44 03	(5)	13	(80)	2° × 2°	T?
104	21 30.4	(4)	50 38	(5)	19	(66)	1°.5 × 1°.5	T?
105	21 35.4	(5)	57 30	(5)	28	(210)	2°.5 × 2°	T
106	22 18.5	(3)	55 58	(3)	31	(190)	4° × 1°	
107	22 22.6	(5)	63 17	(5)	21	(100)	~1°.5	
108	22 56.3	(3)	62 20	(3)	25	(60)	1° × 1°	
109	23 00.3	(4)	58 45	(2)	25	(75)	0°.5 × 1°.5	
110	23 21.2^{+}	(1)	+58 32^{+}	(1)	3120^{+}		P	NT

NOTES TO TABLE II *(Concluded)*

No.
71 Unidentified.
72 Unidentified.
73 W 51, 3C 400? Unidentified. Extended to north.
74 Unidentified.
75 Unidentified.
76 W 55, NGC 6823, emission nebula.
77 Probably emission region, heavily obscured.
78 Faint emission region near source.
79 Unidentified.
80 W 56, UOB 5, unidentified.
81 Cygnus A.
82 W 58, UOB 8, unidentified.
83 UOB 7, unidentified.
84 W 59, unidentified.
85 Unidentified.
86 UOB 12, unidentified.
87 UOB 10, unidentified.
88 W 63, UOB 13, unidentified.
89 Extension of 90.
90 UOB 15*a* (W 64).
91 W 66, HB 20, UOB 14*a*, Sharpless 108, γ Cygni Nebula.
92 W 68*b*, unidentified.
93 W 70, UOB 17, unidentified.
94 Extension of 90? UOB 16.
95 W 71, UOB 19, unidentified.
96 W 75, UOB 20 (UOB 18, W 73, W 72), unidentified.
97 HB 21, supernova remnant.
98 Unidentified.
99 Cygnus Loop, supernova remnant.
100 W 80, UOB 27, NGC 7000, IC 5068, IC 5070.
101 Unidentified.
102 Unidentified.
103 Faint extended emission nebula, Sharpless 119.
104 Perhaps emission nebula, Sharpless 124.
105 HB 22, IC 1396, emission nebula.
106 Possibly extended north to 61°; perhaps emission nebula, Sharpless 132.
107 Unidentified.
108 Unidentified.
109 Unidentified.
110 Supernova remnant.